Journal of Inorganic and Organometallic Polymers and Materials
https://doi.org/10.1007/s10904-020-01448-2

Development of Hybrid TiO_2/Paint Sludge Extracted Microbe Composite for Enhanced Photocatalytic Dye Degradation

V. Santhana[1,2] · D. Thangaraju[1] · A. Tanaka[2] · W. Inami[3] · S. JayaKumar[1] · S. Matsuda[2]

Received: 15 November 2019 / Accepted: 13 January 2020

Abstract
The effect of microbe combination with TiO_2 on photocatalytic degradation of Rhodamine B was investigated. The self-assembled TiO_2 spheres were synthesized by the solvothermal method for preparation of hybrid TiO_2/Paint Sludge Extracted Microbe (PSEM) composite. The structure of as-synthesized TiO_2 was analyzed by the powder X-ray diffraction method, and phase purity was verified with Raman analysis. Spherical morphology and self-assembled nature of TiO_2 was confirmed by field emission scanning electron microscopy (FE-SEM). PSEM extracted from Paint sludge and was used to synthesize TiO_2/PSEM hybrid composite. The dispersion of TiO_2 self-assembled spheres on the walls of PSEM was confirmed with FE-SEM micrographs. TiO_2/PSEM composite (94%) showed enhanced photocatalytic dye degradation when compared with as-synthesized TiO_2 (85%).

Keywords TiO_2 · Microbe · Photocatalysis · Solvothermal growth · Dye degradation · Hybrid composite

1 Introduction

Inadequately treated industrial waste-water discharge is the primary cause of environmental pollution [1]. Adulteration of effluents in the river and ocean leads to critical problems for aquatic ecology [2]. Textile industries dispatch an enormous quantity of synthetic dye mixed wastewater, which brings awful effects on the living species [3, 4]. In past decades, researchers have been searched for efficient and cost-effective solutions to degrade toxic dyes [5]. Photocatalysis is considered as one of the promising methods to solve such environmental problems. Photocatalytic dye degradation process is an environmental friendly method with affordable and less complicated industrial-scale recycling plant establishment [6].

Many inorganic metal oxide semiconductor materials serve as heterogeneous photocatalytic material due to their excellent photo-physical and chemical properties [7, 8]. In which, TiO_2 is one of the finest materials for photocatalytic reactions in all material aspects like suitable bandgap to absorb the UV–Vis region of the solar spectrum and stable chemical properties [9, 10]. A considerable number of research works have been reported after the demonstration of water splitting under light irradiation in the presence of TiO_2 catalyst by Honda–Fujishima group [11]. Bio-compatibility, cost-effective, and high abundant are made TiO_2 as an appropriate material for industrial-grade dye degradation. Many kinds of modifications have been made to enhance the degradation ability, such as noble metal/TiO_2 composite and rare-earth ion-doped TiO_2 [12]. However, research has been still in progress to find the best and model dye degrading catalyst [13–17].

On another hand, microbial dye degradation is also one of the efficient and eco-friendly methods to degrade toxic dyes [18]. Microbes such as algae, yeast, and bacteria were showed a notable result in dye decolorization. Fungi have been showed strong dye degradation ability in the family of microorganisms by self-extraction of ligninolytic enzymes, laccase, lignin peroxidase, and manganese peroxidase [19].

✉ D. Thangaraju
dthangaraju@gmail.com

[1] Nano-Crystal Design and Application Lab (N-DAL), Department of Physics, PSG Institute of Technology and Applied Research, Neelambur, Coimbatore 641 062, India

[2] Graduate School of Integrated Science and Technology, Department of Engineering, Shizuoka University, Hamamatsu 432-8011, Japan

[3] Research Institute of Electronics, Shizuoka University, Hamamatsu 432-8011, Japan

Published online: 24 January 2020

The mechanism behind the fungal dye degradation is the combination of dye adsorption, followed by enzymatic degradation [20]. Fungi have a massive surface area and ease of separation [21]. Binding of inorganic photocatalytic particles with fungi is expected to enhance dye degradation.

In this work, TiO_2 self-assembled spheres were synthesized by the solvothermal method and blended with paint sludge extracted microbe (PSEM). The photocatalytic performance of the synthesized TiO_2/PSEM hybrid composite was investigated using rhodamine B and compared with pure TiO_2.

2 Materials and Methods

2.1 Materials

Titanium (IV) isopropoxide ($Ti(OCH(CH_3)_2)_4$, 95%), n-butanol ($C_4H_{10}O$, 99%), $MnSO_4{\cdot}4H_2O$, KNO_3, NH_4NO_3, $ZnSO_4{\cdot}7H_2O$, Na_2Fe-EDTA$\cdot 2H_2O$, H_2BO_3, $FeSO_4{\cdot}7H_2O$, $CaCl_2{\cdot}2H_2O$, $MgSO_4{\cdot}7H_2O$, KH_2PO_4, Myo-inositol, KI, $Na_2MoO_4{\cdot}2H_2O$, $CuSO_4{\cdot}5H_2O$, $CoCl_2{\cdot}6H_2O$ and Rhodamine B ($C_{28}H_{31}ClN_2O_3$) were purchased from Wako Pure Chemical Industries Ltd, Japan and were utilized without any further purification. De-ionized water was used for all experiments. Melamine resin and paint sludge were purchased from Nisin (Japan).

2.2 Synthesis of TiO_2 Self-Assembled Spheres

TiO_2 spheres were synthesized by the solvothermal method [22]. Titanium (IV) isopropoxide were mixed with n-butanol in a beaker, and 20 mL of de-ionized water was mixed. The mixture was stirred about 60 min for complete hydrolysis of titanium (IV) isopropoxide. Resulting sol was transferred to a 100-mL Teflon-lined stainless-steel autoclave, and heated at 150 °C for 25 h in a temperature-controlled box furnace. As-synthesized particles were separated using centrifugation, and further dried at 150 °C to remove superfluous liquid.

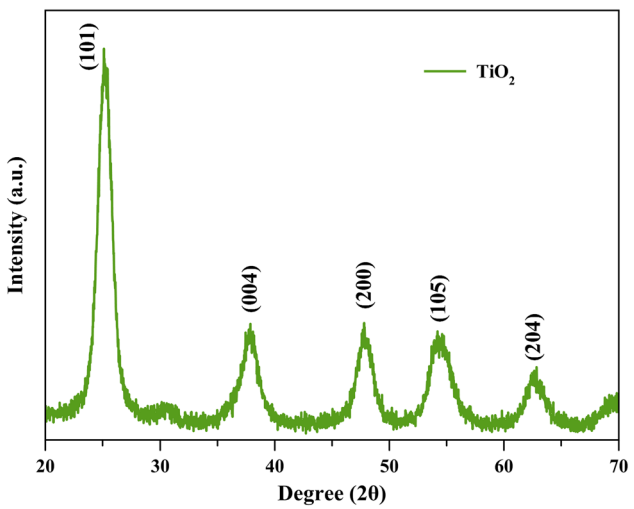

Fig. 1 XRPD pattern of hydro-thermal synthesized TiO_2 particles

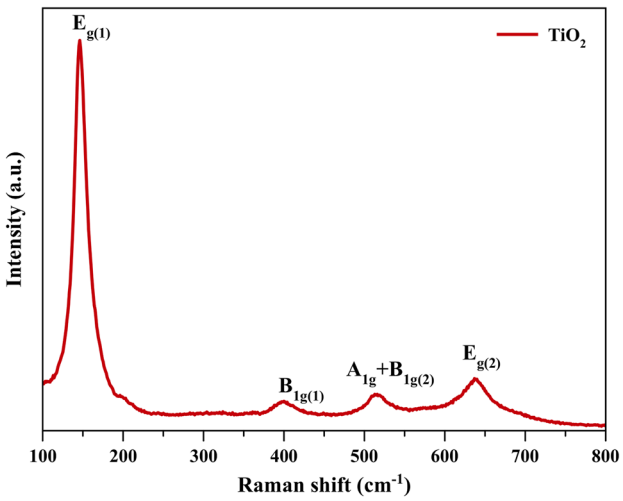

Fig. 2 Raman spectra of hydro-thermal synthesized TiO_2 particles

2.3 Microbe Growth from Paint Sludge

Murashige and Skoog medium (MS) medium was prepared using $MnSO_4{\cdot}4H_2O$ 2.23 g/L, KNO_3 1.9 g/L, NH_4NO_3 1.65 g/L, $ZnSO_4{\cdot}7H_2O$ 0.86 g/L, Na_2Fe-EDTA$\cdot 2H_2O$ 0.75 g/L, H_2BO_3 0.62 g/L, $FeSO_4{\cdot}7H_2O$ 0.56 g/L, $CaCl_2{\cdot}2H_2O$ 0.44 g/L, $MgSO_4{\cdot}7H_2O$ 0.37 g/L, KH_2PO_4 0.17 g/L, myo inositol 0.1 g/L, KI 0.083 g/L, $Na_2MoO_4{\cdot}2H_2O$ 0.025 g/L, $CuSO_4{\cdot}5H_2O$ 0.0025 g/L, $CoCl_2{\cdot}6H_2O$ 0.0025 g/L along with 20 g of agar in a Petri dish. Melamine resin was applied on MS medium, and dried at room temperature for 4–8 h in a clean bench. Paint sludge (3 g) was mixed with 27 mL sterilized water in a homogenizer tool. The derived mixture was homogenized for 10 min with 100 rpm speed. Then, the above solution was further diluted with 27 mL of sterilized water, and this dilution process was repeated for three times. The last dilution was taken for further growth process and was applied to dried melamine resin paint in MS medium. The medium was incubated at 27 °C for a week, and a grown microbe was isolated. Since paint sludge microbial liquid contains various kinds of microbes, only one kind of microbe was identified using colour and shape observation method. Isolated Paint

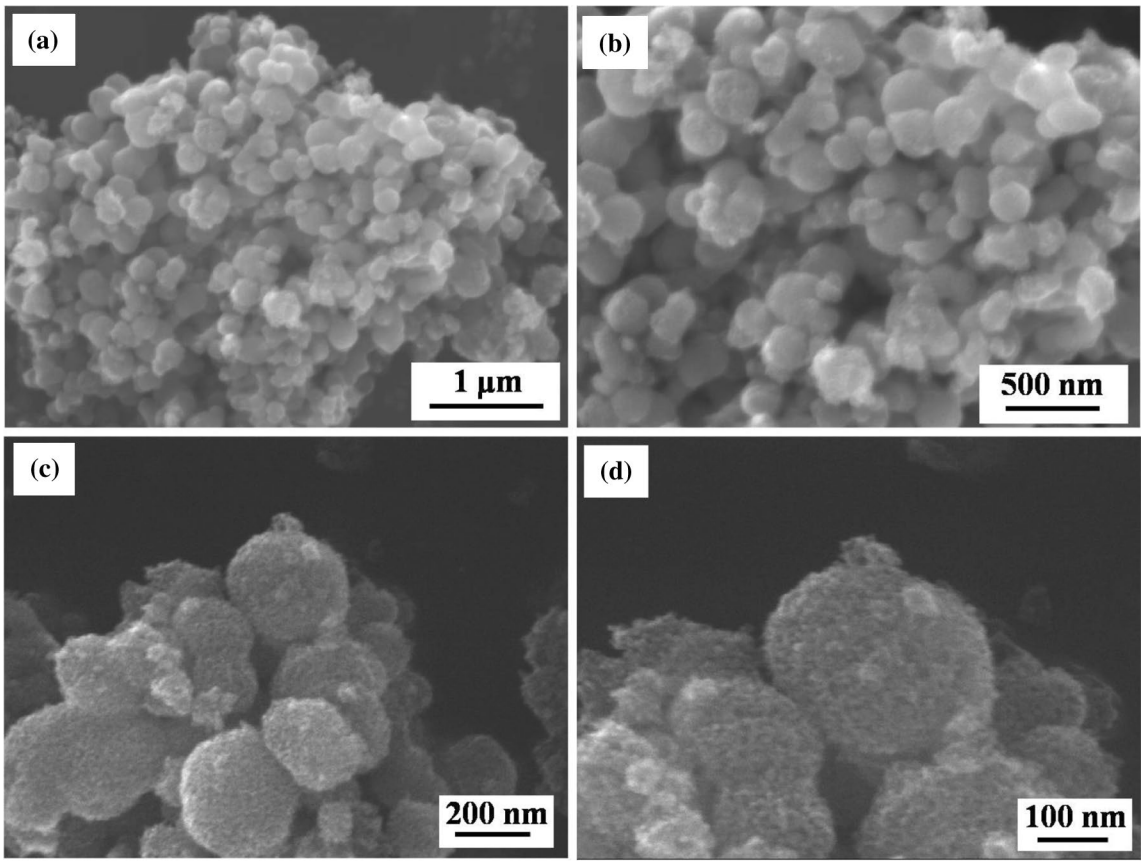

Fig. 3 SEM micrographs of hydro-thermal synthesized TiO_2 self-assembled spheres

Sludge Extracted Microbe (PSEM) was re-grown in a separate MS medium.

2.4 TiO_2/PSEM Hybrid Composite Synthesis

Well grown PSEM was used to make a hybrid composite with self-assembled TiO_2 spheres. Inoculated and cultured PSEM were transferred to liquid nutrient medium (12.5 mL) and were separated from liquid nutrient using a 0.22 mm membrane filter. Further, 25 mL sterilized water was added to the filtered PSEM, and as-synthesized TiO_2 (50 mg) was mixed with PSEM water solution. The hybrid mixture contains 5 Mg of the paint sludge extracted microbe (Filtered using membrane filter) and 50 Mg of the self-assembled TiO_2 nano-spheres. The hybrid mixture was incubated for 30 min for composite formation.

2.5 Photocatalytic Dye Degradation Using TiO_2/PSEM Hybrid Composite

Photocatalytic dye degradation was performed using as-synthesized TiO_2/PSEM composites. Rhodamine B was used to evaluate the degradation ability of bio-catalytic composite. Dye degradations experiments were performed using a glass reactor (SANSYO Tokyo) with water-circulating outer jacket. TiO_2 and TiO_2/PSEM were dispersed in 50 mL of dye (10 mg/L) solution and was irradiated with a white light source (500 W, HATAYA). Uniform distance (11 cm) was maintained between the reactor bottom and light source for all experiments. At constant time intervals (10 min), 5 mL of solution was withdrawn from the reaction mixture and centrifuged to remove the suspended catalyst. The concentration of dye was measured with UV–VIS absorption.

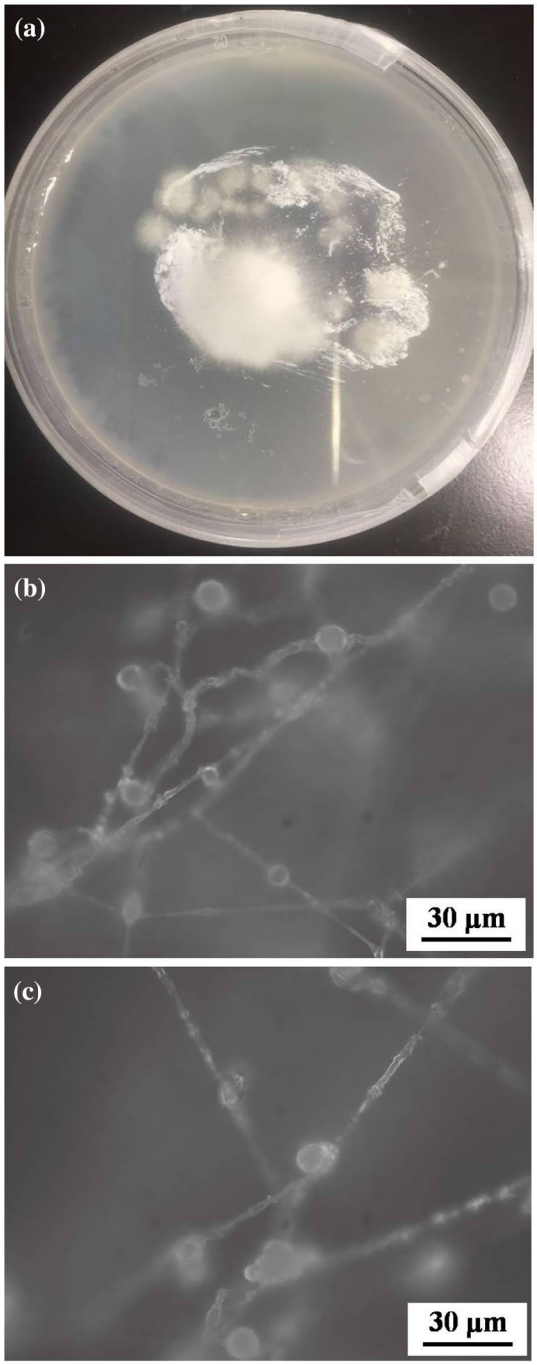

Fig. 4 Micrographs of PSEM growth on melamine resin coated MS medium (**a**) and micrographs of grown microbes (**b** and **c**)

2.6 Characterization

As-prepared TiO_2 powder was examined by RINT-2200 Rigaku X-ray powder diffractometer (Cu-Ka radiation, $\lambda = 1.54178$ A) (XRPD) at a scan rate of 0.048 s^{-1} in the 2θ range of 20° to 80°. Raman spectrum was recorded in the range of 100–1000 cm^{-1} by a Jasco NRS-7100 Raman spectrophotometer. TiO_2 morphology was examined by field-emission scanning electron microscope (FE-SEM) (JEOL JSM6320F, Japan). Upright Olympus digital microscopes were used to examine as-grown PSEM. Hybrid TiO_2/PSEM composite was grown on metal sheet, and its morphology was recorded using JEOL JSM-7001 Field emission scanning electron microscope (FE-SEM), Japan. The degraded dye absorption percentage was evaluated in the range of 200–800 nm using a JascoV-670 UV/Vis–NIR spectrophotometer.

3 Result and Discussion

3.1 Hydro-Thermal Grown TiO_2 Self-Assembled Spheres

The product crystal structure was evaluated by the XRPD method, as shown in Fig. 1. Five well resolved XRPD reflection peaks were well matched with pure anatase titania phase (JCPDS Card No. 21–1272) without impurity. Scherrer's formula was used to calculate average crystallite size using the most intense anatase (101) peak [23].

$$D = \frac{k\lambda}{\beta cos\theta} \tag{1}$$

Where λ is the wavelength of X-ray, β is the full width half maximum, θ is the Bragg's angle, K is constant (0.0889), and D is the average particle size. The calculated average particle size was 2.8 nm.

Raman spectra of as-synthesized TiO_2 is shown in Fig. 2. Four Raman bands were observed at 147, 398, 516, and 641 cm^{-1}, which corresponds to Eg(1), B1g(1), A1g + B1g(2), and Eg(2) modes, respectively. Observed modes were attributed that synthesized TiO_2 belongs to anatase titania. Sharp intensity bands revealed crystalline nature of the TiO_2 powder [24].

As-synthesized samples were undergone SEM investigation to understand morphology and surface structure. Figure 3a–d shows SEM micrographs of as-synthesized TiO_2. Sphere-like morphology was observed with size ranging between 100–300 nm. The self-assembled spongy-like surface was recognized from the higher resolution images. Calculated crystalline size using Scherrer's formula was well

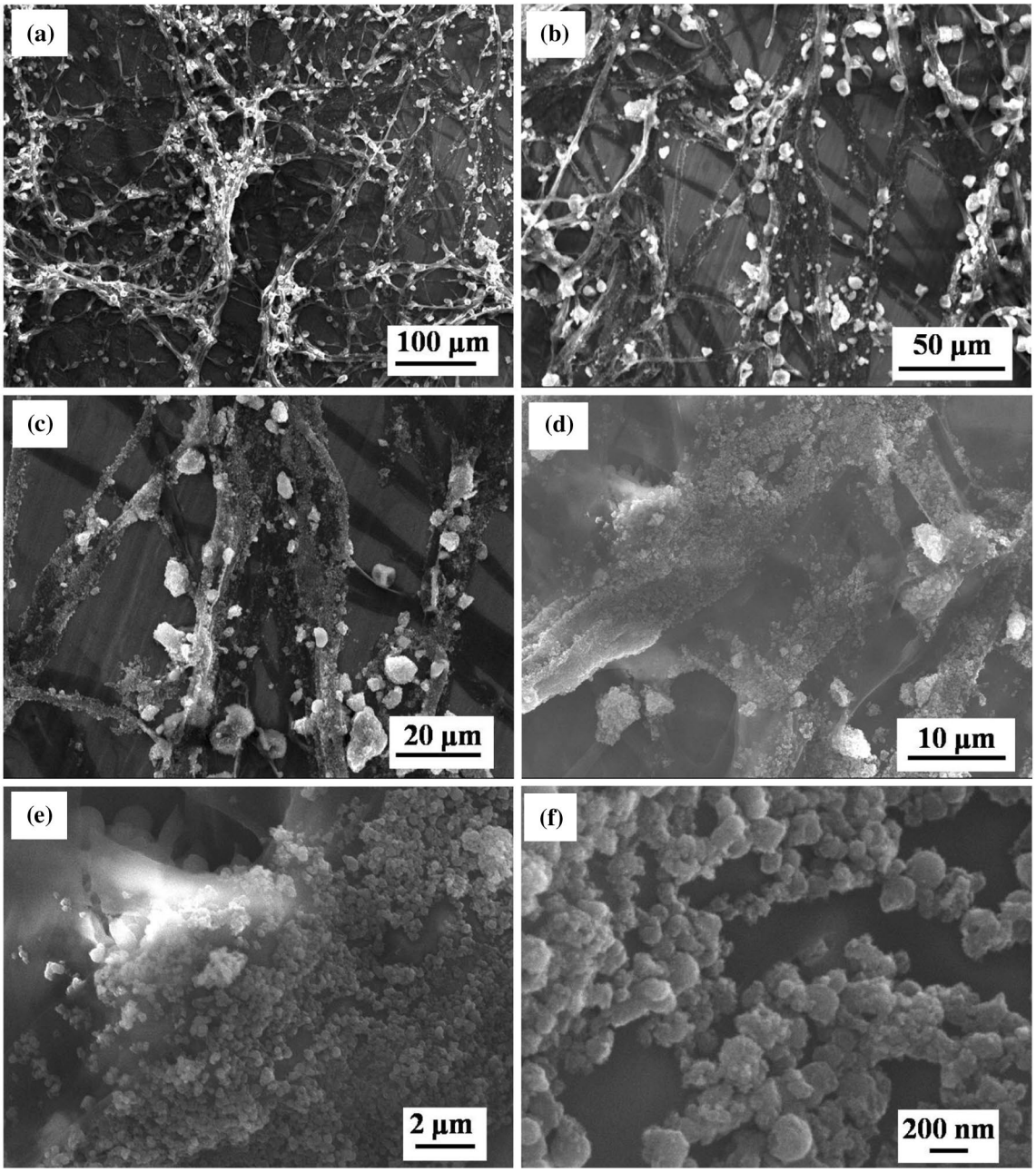

Fig. 5 FE-SEM micrographs of TiO_2/PSEM composite on metal plate

agreed with formation of self-assembled spheres consists of several small nanoparticles.

3.2 TiO_2/PSEM Hybrid Composite

Figure 4a shows the isolated growth of microbes on melamine resin in MS medium. Sphere-like conidia connected with foot cells was observed (Fig. 4b, c). Growth format and appearance indicate that a grown microbe is fungi. The well-branched hyphae from foot cells were observed, and the spherical shape of conidia is connected through conidiophores with them. The observed shape of fungi suggests that it may be the aspergillus genus [25].

The formation of hybrid TiO_2/PSEM composite was further confirmed with the FE-SEM micrograph, as shown in

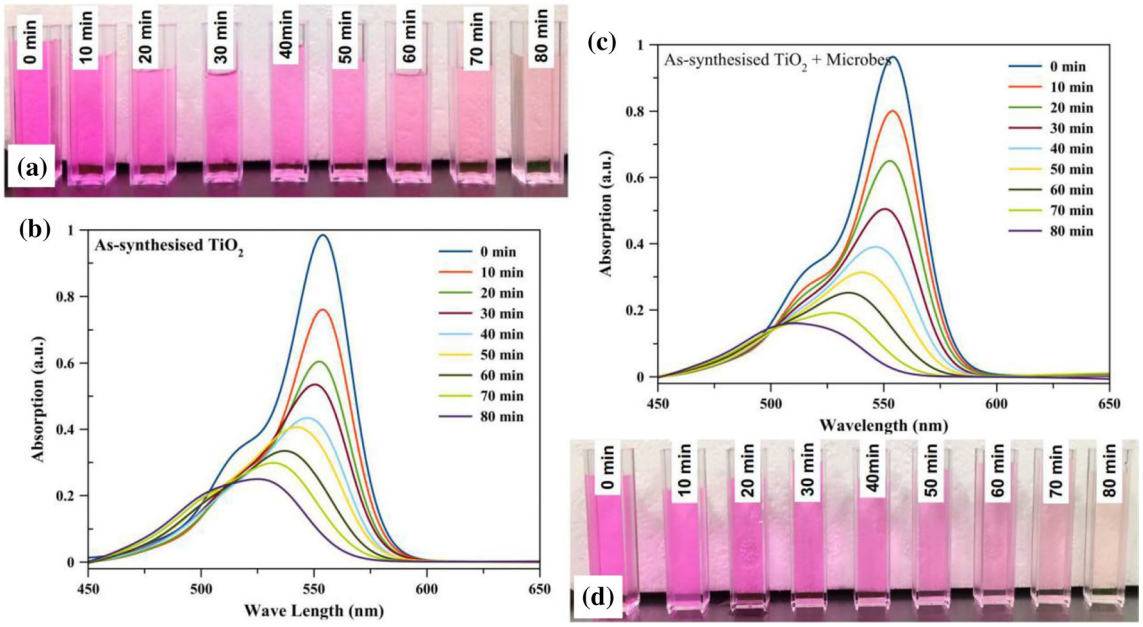

Fig. 6 Comparison of rhodamine B degradation solution (**a**), UV–Vis absorption (**b**) of as-synthesized TiO_2, and UV–Vis absorption (**c**) and comparison (**d**) of TiO_2/PSEM composite

Fig. 5a–f. Self-assembled TiO_2 nanospheres bind on fungal hyphae. Figure 5a and b indicates that conidias were connected to foot cells through conidiospores, which is well agreed with the microscope images. The sizes of observed conidia were between 10 and 20 µm. Well-dispersed TiO_2 sphere-like particles appeared on the walls of foot cells, as depicted in Fig. 5c–f.

3.3 Dye Degradation Experiment

As-synthesized TiO_2 and TiO_2/PSEM composites were used to evaluate the photocatalytic ability by the degradation of rhodamine B upon irradiation of white light. The absorbance of rhodamine B of TiO_2 and TiO_2/PSEM composite was gradually decreased at constant time intervals. Visual and UV–Visible comparison of dye degradation was presented in Fig. 6a, b, c, and d. A high-intensity peak at 554 nm was representative absorption of rhodamine B, and intensity was gently decreased. Peak position was shifted towards 498 nm, which indicates oxidation and reduction of rhodamine B occurred under light photon irradiation on semiconducting TiO_2.

Performance of as-synthesized TiO_2 and TiO_2/PSEM was recorded 80 min with an interval of 10 min. Photocatalytic dye degradation performance of TiO_2/PSEM hybrid composite showed higher activity than as-synthesized TiO_2. Experiments were performed only with PSEM under dark and the presence of light to investigate the role of PSEM in the dye degradation. The results are presented in Fig. 7a, b, and c. The PSEM microbes only showed higher de-colorization under light condition than that of dark, which confirms the light activeness of these microbes. Nominal de-colorization PSEM under dark condition may be due to the adsorption of rhodamine B and was nominally increased under light condition. The composite TiO_2/ PSEM under light irradiation showed considerable enhancement in dye degradation than that of as-synthesized TiO_2.

The rhodamine B degradation percentage was determined by the following Eq. (2)

$$\text{Rhodamine B degradation percentage} = \frac{A_0 - A_t}{A_0} \times 100 \quad (2)$$

Here, A_0 and A_t represent the initial absorbance and absorbance at time t, respectively. Calculated percentage of dye degradation of PSEM under dark, PSEM under light, as-synthesized TiO_2, Hybrid TiO_2/PSEM composite under light and dark at 70 min of light irradiation is 7, 16, 85, 94 and 11%, respectively as compared in Fig. 8. Percentage of rhodamine B degradation comparison gives

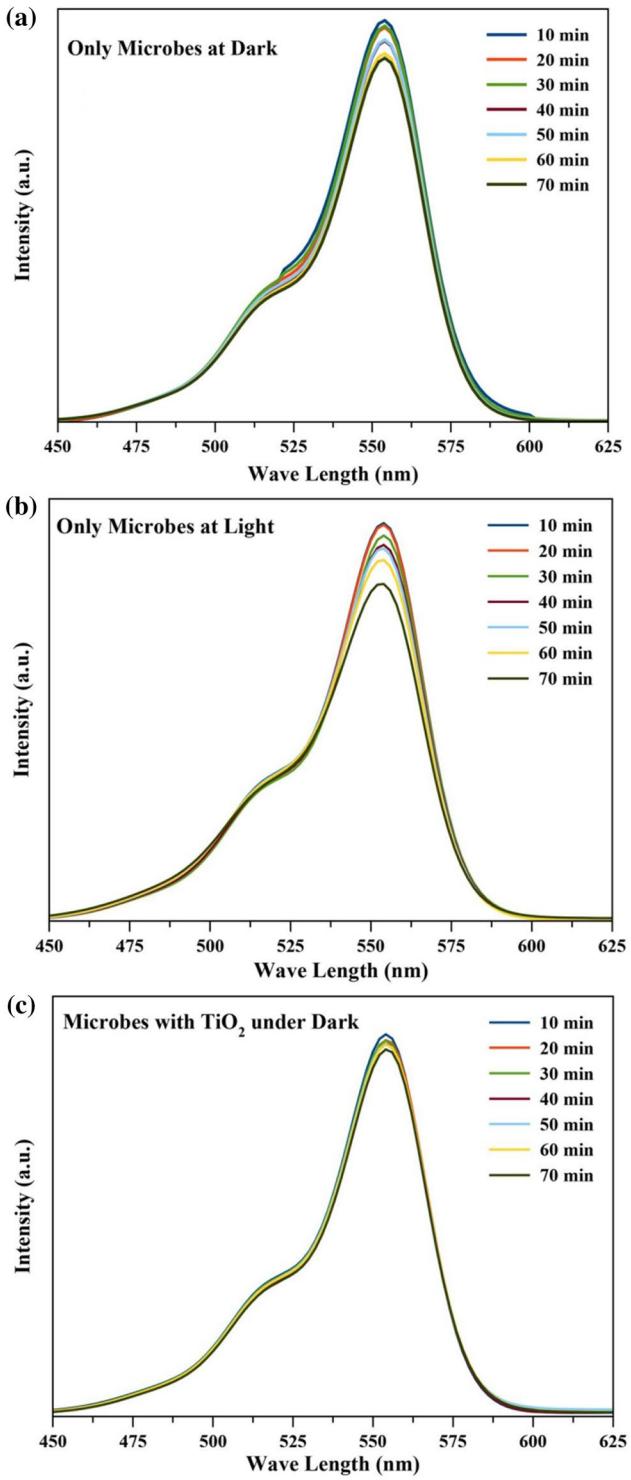

Fig. 7 UV–Vis spectral comparison of rhodamine B degradation to time using only microbes at dark (**a**), only microbes at white light (**b**) and TiO_2/PSEM composite at dark (**c**)

a clear idea about the possibilities of enhanced activity of TiO_2/PSEM hybrid composite. The degradation activity of PSEM under light was two times higher than that of PSEM under dark conditions. The above result was reflected in PSEM along with the TiO_2 composite. The activity showed 10% excess degradation than as-synthesized TiO_2. Dye degradation of TiO_2/PSEM reached 98% of dye degradation at 80 min under white light irradiation, which is remarkably high degradation of TiO_2/PSEM composite.

Rate of photocatalytic dye degradation by TiO_2 and TiO_2/PSEM hybrid composites follows a pseudo-first-order reaction given in Eq. (3)

$$ln\left(\frac{C_0}{C}\right) = kt \tag{3}$$

$$t_{1/2} = \frac{\ln 2}{k} \tag{4}$$

Here, k is the pseudo-first-order rate constant, C_0, and C are the initial and final concentration of rhodamine B, respectively. Concentrations were calculated based on Beer-lambert's law from UV–Visible absorption values at 554 nm [26]. The plot between $ln(C_0/C)$ and degradation time is presented in Fig. 9.

The rate constant was calculated for the samples by taking of slope of a fit line. The calculated rate and half lifetime using Eq. (4) were compared in Table 1. Among them, TiO_2/PSEM under white light has shown a higher rate of decomposition as well as low half-life time when compared with the as-synthesized sample.

Higher degradation results of the present hybrid structure were well agreed with the previously reported TiO_2/carbon and TiO_2/polymer hybrid fiber structures [27, 28]. Proper coating of TiO_2 material on the surface of the carbon fiber leads both carbon and the TiO_2 to take part in the degradation of dyes. The same scenario happens in the current synthesized organic/inorganic hybrid TiO_2/PSEM. In hybrid structure, TiO_2 spheres were decorated on the surface of the PSEM, which leads the participation of both TiO_2 spheres and PSEM in the degradation process of dye under the light. Exposure of TiO_2 and microbe surface to the dye solution may be the reason for the overall increment in the dye degradation percentage and rate in the TiO_2/PSEM composite when compared with TiO_2 spheres alone.

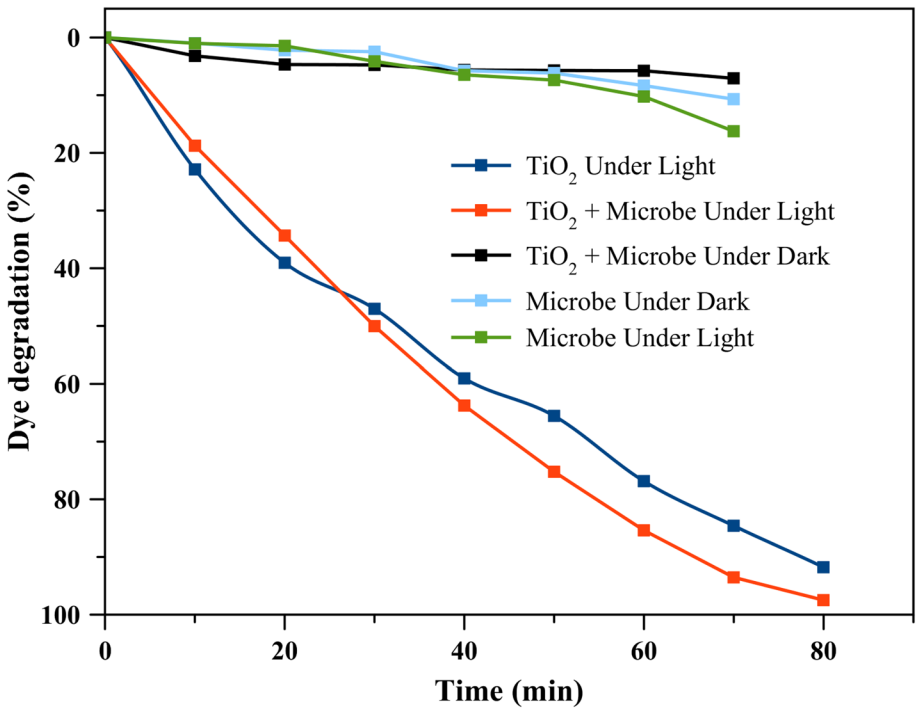

Fig. 8 Comparative rhodamine B degradation percentage using as-synthesized TiO_2, TiO_2/PSEM under light, TiO_2/PSEM under dark, only microbes under dark and light

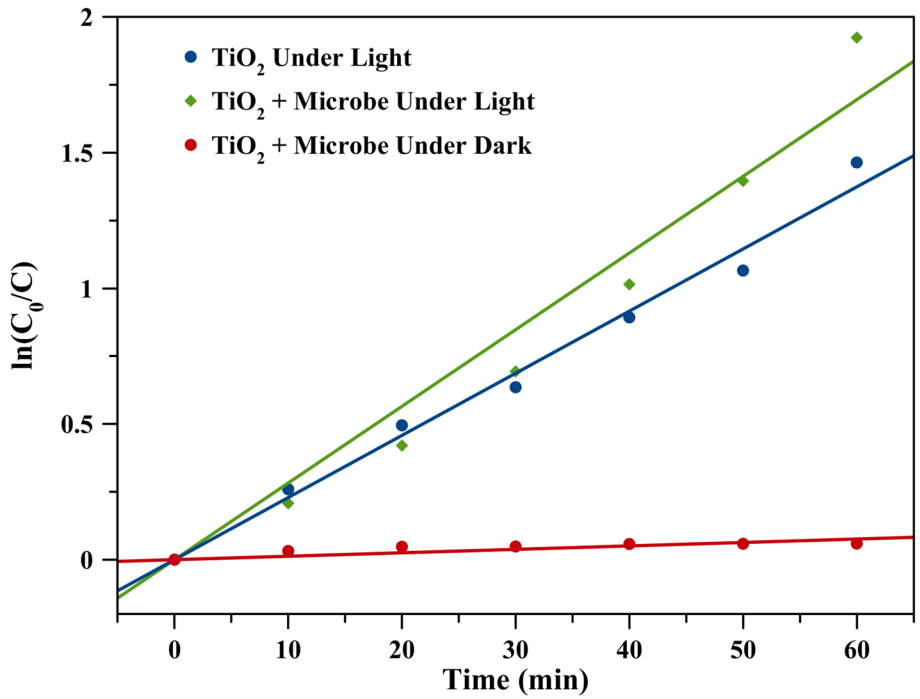

Fig. 9 A plot between $\ln(C_0/C)$ and time of as-synthesized TiO_2 under light, TiO_2/PSEM under light, and dark

Table 1 Calculation of pseudo-first-order rate constant and a half life-time of Rhodamine B degradation for pure TiO_2, TiO_2/PSEM under light

S. No	Sample name	Pseudo-first-order rate (k) (min^{-1})	Half-life ($t_{1/2}$) (min)
1	TiO_2 under light	0.022	31.50
2	TiO_2/PSEM under light	0.028	24.75

4 Conclusion

The PSEM was successfully extracted from paint sludge, and hybrid TiO_2/PSEM composite was prepared using solvothermal synthesized TiO_2 spheres. Anatase structure of as-synthesized TiO_2 nanostructure was confirmed with the powder XRD method, and phase purity was verified

with Raman analysis. SEM micrographs revealed that the spherical morphology and self-assembled nature of the TiO_2 powder. The TiO_2 spheres decorated PSEM composite was confirmed with FESEM analysis. Photocatalytic experiment results indicate that the dye degradation rate of hybrid TiO_2/PSEM composite is higher than that of pure TiO_2.

Acknowledgement One of the authors (VEDI Santhana) thanks Asia bridge program (ABP), Shizuoka University, Hamamatsu Japan. The author (D. Thangaraju) sincerely thanks Science and Engineering Research Board (ECR/2017/002974), Department of Science and Technology, Government of India, for the financial support.

References

1. M. Pelaez, N.T. Nolanb, S.C. Pillai, M.K. Seery, P. Falaras, A.G. Kontos, P.S.M. Dunlop, J.W.J. Hamilton, J.Anthony Byrne, K. O'Shea, M.H. Entezari, D.D. Dionysiou, Appl. Catal. B Environ. **125**, 331 (2012)
2. R.C. Miranda, E.B. Gomes, N. Pereira Jr., M.A.M. Morales, K.M. Machado, N.B. Gusmao, Bioresour. Technol. **142**, 361 (2013)
3. X.C. Jin, G.Q. Liu, Z.H. Xu, W.Y. Tao, Appl. Microbiol. Biotechnol. **74**, 239 (2007)
4. R.G. Saratale, S.S. Gandhi, M.V. Purankar, M.B. Kurade, S.P. Govindwar, S.E. Oh, G.D. Saratale, J. Biosci. Bioeng. **115**, 658 (2013)
5. N. Prakash, D. Thangaraju, R. Karthikeyan, M. Arivanandhan, Y. Shimura, Y. Hayakawa, RSC Adv. **6**, 80655 (2016)
6. H. Wang, L. Zhang, Z. Chen, J. Hu, S. Li, Z. Wang, J. Liu, X. Wang, Chem. Soc. Rev. **43**, 5234 (2014)
7. M.R. Hoffmann, S.T. Martin, W. Choi, D.W. Bahnemannt, Chem. Rev. **95**, 69 (1995)
8. K. Omri, R. Lahouli, J. Mater. Sci.: Mater. Electron. **30**, 7834 (2019)
9. K. Hashimoto, H. Irie, A. Fujishima, Jpn. J. Appl. Phys. **44**, 8269 (2005)
10. X. Chen, S.S. Mao, Chem. Rev. **107**, 2891 (2007)
11. A. Fujishima, K. Honda, Nature **238**, 37 (1972)
12. J. Schneider, M. Matsuoka, M. Takeuchi, J. Zhang, Y. Horiuchi, M. Anpo, D.W. Bahnemann, Chem. Rev. **114**, 9919 (2014)
13. A.R. Daghrir, P. Drogui, D. Robert, Ind. Eng. Chem. Res. **52**, 3581 (2013)
14. Y.F. Li, D. Xu, J.I. Oh, W. Shen, X. Li, Y. Yu, ACS Catal. **2**, 391 (2012)
15. K. Omri, N. Alonizan, J. Inorg. Organomet. Polym. Mater. **29**, 203 (2019)
16. K. Omri, N. Alonizan, Appl. Phys. A **125**, 696 (2019)
17. N. Prakash, D. Thangaraju, R. Karthikeyan, M. Arivanandhan, Y. Shimura, Y. Hayakawa, RSC Adv. **84**, 80655 (2016)
18. P. Kaushik, A. Malik, Environ. Int. **35**, 127 (2009)
19. S.K. Sudip, R. Smita, B. Partha, R. Sangeetha, Fungal Biol. Rev. **30**, 112 (2016)
20. N. Gomi, S. Yoshida, K. Matsumoto, M. Okudomi, H. Konno, T. Hisabori, Y. Sugano, Biodegradation **22**, 1239 (2011)
21. A. Mishra, A. Malik, Crit. Rev. Environ. Sci. Technol. **43**, 1162 (2013)
22. N. Prakash, R. Karthikeyan, D. Thangaraju, M. Navaneethan, M. Arivanandhan, T. Koyama, Y. Hayakawa, ChemPhyChem **16**, 3084 (2015)
23. S. R. Sani, F. Mohseni, M. Javid, A. Mortezaali, Eur. Phys. J. Plus 131, 370 (2016).
24. X. Yang, Y. Wang, L. Xu, X. Yu, Y. Guo, J. Phys. Chem. C **112**, 11481 (2008)
25. C.V. Sciortino Jr., *Atlas of Clinically Important Fungi* (John Wiley & Sons, Inc., New Jersey, 2017)
26. S. Rasalingam, C.M. Wu, R.T. Koodali, A.C.S. Appl, Mater. Interfaces **7**, 4368 (2015)
27. Y. Xie, Z. Pan, Z. Wei, W. Feng, J. Zuo, G. Hu, C. Xiao, Advanced Materials Research **631**, 176 (2013)
28. Z. Chu, L. Qiu, Y. Chen, Z. Zhuang, P. Du, J. Xiong, J. Phys. Chem. Solids **136**, 109138 (2020)